

# CFD Based Aerodynamics Conjugate Heat Transfer and Airgap Fluid Flow Thermal Analysis to a Wheel Hub Motor for Electric Scooters

Mambazhasseri Divakaran, A., Abo-Serie, E., Gkanas, E., Jewkes, J. & Shepherd, S

Published PDF deposited in Coventry University's Repository

## Original citation:

Mambazhasseri Divakaran, A, Abo-Serie, E, Gkanas, E, Jewkes, J & Shepherd, S 2023, CFD Based Aerodynamics Conjugate Heat Transfer and Airgap Fluid Flow Thermal Analysis to a Wheel Hub Motor for Electric Scooters. in JD Nixon, A Al-Habaibeh, V Vukovic & A Asthana (eds), Energy and Sustainable Futures: Proceedings of the 3rd ICESF, 2022. Springer Proceedings in Energy, Springer , pp. 21-29, 3rd International Conference on Energy and Sustainable Futures (ICESF) , Coventry, United Kingdom, 7/09/22. [https://doi.org/10.1007/978-3-031-30960-1\\_3](https://doi.org/10.1007/978-3-031-30960-1_3)

DOI 10.1007/978-3-031-30960-1\_3

ISSN 2352-2534

ESSN 2352-2542

Publisher: Springer

This chapter is licensed under the terms of the Creative Commons Attribution 4.0 International License (<http://creativecommons.org/licenses/by/4.0/>), which permits use, sharing, adaptation, distribution and reproduction in any medium or format, as long as you give appropriate credit to the original author(s) and the source, provide a link to the Creative Commons license and indicate if changes were made.

The images or other third party material in this chapter are included in the chapter's Creative Commons license, unless indicated otherwise in a credit line to the material. If material is not included in the chapter's Creative Commons license and your intended use is not permitted by statutory regulation or exceeds the permitted use, you will need to obtain permission directly from the copyright holder.

# Chapter 3

## CFD Based Aerodynamics Conjugate Heat Transfer and Airgap Fluid Flow Thermal Analysis to a Wheel Hub Motor for Electric Scooters



A. M. Divakaran, E. Abo-Serie, E. I. Gkanas, J. Jewkes, and S. Shepherd

**Abstract** The geometry of commercially available wheel hub motors inherently restricts packaging space and may prevent the introduction of more sophisticated, efficient, and expensive cooling systems. Due to the limited available space in the wheels, commercial hub motors often rely on aerodynamic passive cooling. The small air-gap (0.5–1 mm) between the coils and the magnets results in heat transfer to the magnets and consequently increases their temperature. As a result, the performance of the permanent magnets (PMs) will be limited and also will heavily affect their lifetime; thus, advanced cooling strategies must be introduced. In the current study, a three-dimensional (3D) thermal model was developed for a commercially available 500 W scooter hub motor under a constant heat load of 180 W using Computational Fluid Dynamics (CFD) (= 64%). The spatial distribution of the temperature for the motor parts are evaluated considering both the internal and external fluid flow dynamics. Further, analysis of airflow in the the gap is performed and the results from the CFD is compared with the published correlations. The flow in such small motor was found to be laminar with Taylor number below 40. Results also showed that enhancement of the cooling is necessary to avoid damage of the winding vernish and to reduce the magnets temperature particularly when the motor works at high torque with low efficiency.

**Keywords** Thermal management · Computational fluid dynamics · Taylor's correlations · Outer-rotor machines

---

A. M. Divakaran (✉) · E. I. Gkanas · S. Shepherd  
Institute of Future Transport and Cities, Centre for Advanced Low Carbon Propulsion System,  
Coventry University, Coventry, UK  
e-mail: [mambazhasa@uni.coventry.ac.uk](mailto:mambazhasa@uni.coventry.ac.uk)

E. Abo-Serie · J. Jewkes  
School of Engineering, The University of Leicester, Leicester, UK

### 3.1 Introduction

An effective thermal management system can improve the efficiency, stability, and lifespan of the traction motors used in electric vehicles. So, it is essential to study and evaluate the cooling performance of such machines at different operating conditions. PM based brushless DC wheel hub motors have many advantages such as higher efficiency and power density, simplified transmission link, better power output control, and more space in the vehicles. Nevertheless having effective cooling is one of the major challenges [1]. A significant number of publications are available on the various cooling techniques used in electrical machines but very few on cooling wheel hub motors [2–4]. The techniques focus on ensuring adequate heat dissipation from the electric coils as a source of heat to the surrounding air by creating low thermal resistance path that should be away from the magnets locations for the heat to be dissipated. Effective cooling helps to achieve the cooling system goal of lowering the temperature of the sensitive components such as the windings and PMs, and also the bearings [5]. The hub motor heat transmission was successfully modeled by Fasil et al. [6] using computational fluid dynamics (CFD), finite element (FE), and lumped parameter (LP) models investigated the heat dissipation in wheel hub motor. They used LP model to calculate the temperature of the components in the motor and validated it with the FE method and CFD for investigating the internal and external flow analysis and convective heat transfer for the wheel motor. The electrical machines can be broadly classified into two major types, totally enclosed and ventilated and the cooling need to be adjust for each type. Air-gap is a very important parameter for motor performance and it is not possible to change for cooling purposes. However, the characteristics of the flow and heat flux distribution is very crucial as it can affect the performance of the magnets. Depending on the motor size and operating conditions, the size of the air-gap between the stator and the rotor varies for different types of machines. Small or light duty machines have a small airgap (0.5–1 mm) to reduce electromagnetic losses, while heavy duty machines have a large air gap to lessen drag due to the high magnetic field [7]. It is difficult to capture the physics of fluid flow in an airgap, however there have been efforts towards the development of empirical correlations for both the spinning inner cylinder and stationary outer cylinder [8, 9]. Effective thermal management, or how well the temperature is kept below the thermal limit of the PMs (150 °C), determines the machine's lifespan and performance [8].

The flow characteristics in the air gap region of cylindrical machines can be determined with the non-dimensional Taylor number ( $Ta$ ). The Taylor number provides a relative effect of inertial and viscous force for annulus fluid flow between rotating cylindrical surfaces. When the fluid flow dynamics is laminar, conduction is only the mode of heat transfer in the air gap for low-speed operation ranges below 1000 RPM. The creation of vortices and turbulent flow, which appear at 1300 RPM and 4600 RPM, results in an increase in heat transfer (for a 1 mm air gap). When the  $Ta$

is less than 41, the flow is laminar, and the “Nu” is 2, indicating that heat transfer is only with conduction and when the  $Ta$  is between 41 and 100, when the flow changes to a vortex, and when the  $Ta$  is greater than 100, the flow becomes turbulent [9].

Howey and Holmes [8] reviewed the nondimensional parameters for both the cylindrical and disc-type machines with worked-out examples. The main outcome of this study was that for accurate thermal modelling of the electrical machines the knowledge of surface or air gap convective heat transfer is essential. On another study the authors reviewed many non-dimensional parameters and most commonly used heat transfer correlations for various gap sizes [9]. They also highlighted the effect of slots on the cylindrical surface to the non-dimensional numbers in comparison with a smooth cylinder of the same size. Considering this, Hosain et al. [10] investigated the effect of Taylor vortices on the heat transfer in the air gap region for a cylindrical inner rotor machine. They validated the numerical simulation results with the empirical correlation results and pinpointed the periodic temperature and heat transfer pattern. The air gap in axial flux motors represents heat transfer between two concentric cylinders, many published literature can be found representing the inner cylinder rotating and stationary outer cylinder [11]. But in hub motors, the outer cylinder is rotating and the inner cylinder is stationary. In [8], the authors reviewed the correlations for dimensionless quantities, cylindrical machines and disc-type machines. However, the application of these correlation to estimate the non dimensional quantities in the air-gap for a wheel hub brushless dc machine has not been investigated.

In this paper, a wheel hub motor commonly used in electric scooters has been investigated for conjugate heat transfer for a steady state heat loss of 180 W in the windings. The continuous power rating and electrical specification of the motor is 500 W, 3-phase 48 V. The topology of the hub motor is outer rotor axial flux PM brushless DC machine, Figs. 3.1a and 3.2a. The stator core consist of windings and the shaft and the rotor comprises of permanent magnets, sleeve and rotor body. An air-gap of 0.5 mm exists between the rotor and and stator. A computational fluid dynamics (CFD) based study has been carried out to assess the heat transfer from the winding (source) to the ambient air and to investigate the small air-gap fluid flow. Nusselt number (Nu) and heat transfer coefficient at the air gap has determined numerically with CFD analysis, and compared, validated with the correlations in the published literature.

## 3.2 Methodology

The design geometry used in the current study is for conjugate heat transfer assessment and verification, which resembles a small wheel hub motor used in electric scooters. The purpose of using the complete design geometry of the motor is to investigate the heat transfer mechanism in the wheel hub motor and to determine the heat transfer coefficient on the rotor surface. The components of the motor geometry considered for the setting up the thermal model has all the components as shown in Fig. 3.1. Conformal meshing is achieved with a polyhedral prism layer mesh, the

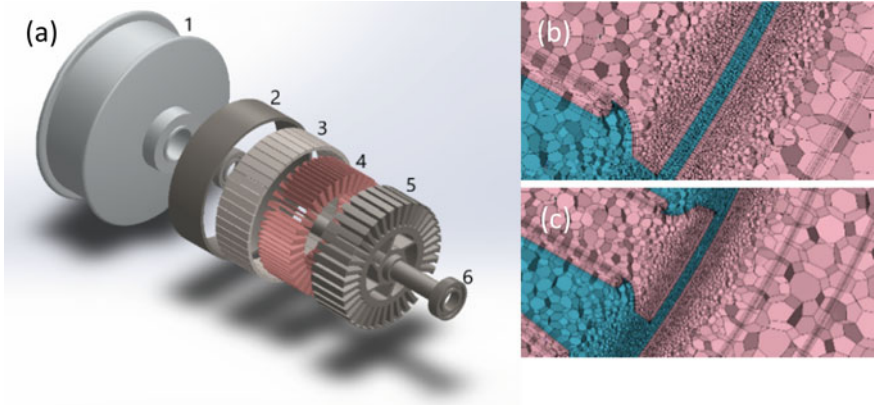


**Fig. 3.1** Shows the geometry of the motor considered for the simulation **a** 3D CAD exploded view 1. Rotor 2. Rotor sleeve or rotor core 3. PMs 4. Windings 5. Stator and shaft 6. Bearings, **b, c** Small section of meshing the fluid and solid domain with air gap refinement (33 million cells)

mesh domain contains 33 million cells with very fine prism layers at the solid–fluid interface and the air-gap region, Fig. 3.1b, c. The computational domain includes the external fluid domain, rotating region, internal fluid and solid domain, and the components of the motor are shown in 3.2b. The motor stator consists of the motor windings, stator and shaft and the rotor consist of a permanent magnet, sleeve, rotor and bearings. A rotating region is created around the rotor that rotates at a speed of 482 rpm with no-slip boundary conditions at the solid–fluid interfaces.

The rotational reference frame is set at the appropriate solid–fluid interface with no-slip boundary conditions to generate the velocity gradient. Both internal and external fluid flow are considered in the simulation to make the conjugate heat transfer simulation analysis more realistic. Outer walls of the ambient fluid domain are set at a velocity inlet (0.5 m/s), pressure outlet, and convection boundary conditions (20 °C, 20 W/m<sup>2</sup>K). A constant heat generation of 180W is assigned to the copper winding as one block which is calculated based on total heat loss in the motor (assuming  $\eta=64\%$ ). This is considered as a worst case scenario. Steady-state Realizable k-epsilon turbulence model with coupled solid energy physics was used to model the turbulence together with enhanced wall treatment. A mesh independent study was performed at an early stage of this study.

To compare CFD results in the air-gap the following dimensionless parameters have been used [5]

$$Nu = \frac{hD_h}{k} \quad (3.1)$$

$$T_{am} = \frac{\omega_a R_m^{0.5} (b-a)^{1.5}}{v} \quad (3.2)$$

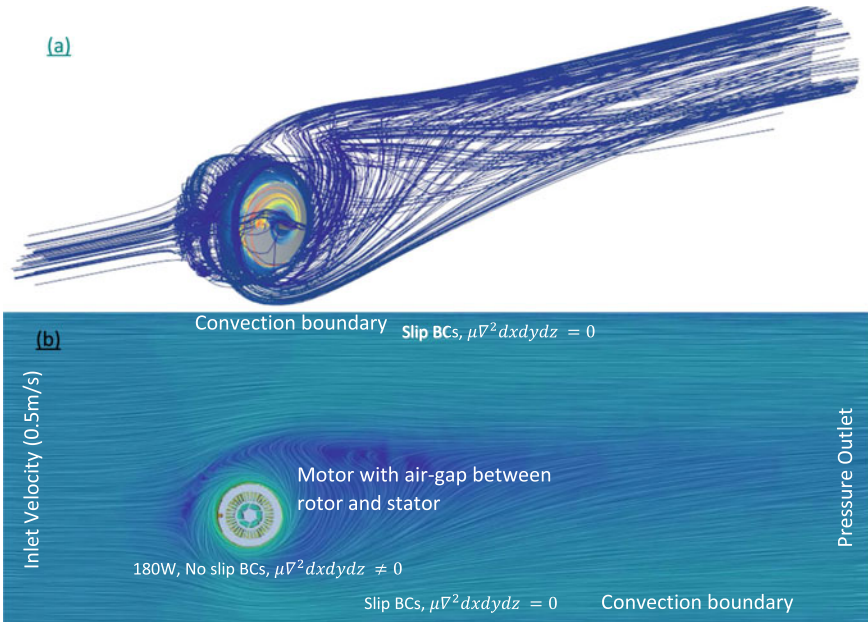


**Fig. 3.2** Shows the simulation domain and fluid flow. **a** Streamlines on the external motor surface **b** Shows the simulation domain with boundary conditions (whole domain resulted in 33 Million cells)

$$F_g = \frac{\pi^2}{41.19\sqrt{S}} \left( 1 - \frac{(b-a)}{2R_m} \right) \tag{3.3}$$

$$S = 0.0571 \left( 1 - 0.652 \frac{\frac{(b-a)}{R_m}}{1 - \frac{(b-a)}{2R_m}} \right) + 0.00056 \left( 1 - 0.652 \frac{\frac{(b-a)}{R_m}}{1 - \frac{(b-a)}{2R_m}} \right)^{-1} \tag{3.4}$$

$$\frac{T_{am}^2}{F_g^2} < 1700; \text{ the flow is laminar} \tag{3.5}$$

$$1700 < \frac{T_{am}^2}{F_g^2} < 10^4; \text{ the flow is laminar with vortices} \tag{3.6}$$

where,  $T_{am}$  is the Taylor number,  $Nu$ —Nusselt number,  $h$ —heat transfer coefficient ( $W/m^2K$ ),  $D_h$ —hydraulic diameter (m),  $\omega_a$ —angular speed in rad/sec,  $k$ —thermal conductivity ( $W/mK$ ),  $R_m$ —mean radius ( $(a + b)/2$ ),  $b$ —outer cylinder radius (m),  $a$ —inner cylinder radius (m),  $F_g$ —geometric factor.

### 3.3 Results and Discussion

When the heat loss in the winding is 180 W ( $\eta = 64\%$ ) at 482 RPM, the maximum temperature in the winding was 325 °C. The temperature drops to 266 °C when the speed of the motor doubled (964 rpm) as shown in Fig. 3.3a, b . The maximum temperature in the winding is beyond the thermal limit of all the classes of insulation materials available in the market (maximum hotpoint temperature 240 °C). The temperature rise beyond the thermal limit damages the insulation and also results in demagnetization of the PMs [12]. Clearly this mode of motor operation at low rpm and low efficiency require an efficient thermal management system. The heat transfer coefficient ( $h$ ) for the rotor surface is found to vary between 0-175 W/m<sup>2</sup>K at 482 rpm and 0-330 W/m<sup>2</sup>K at 964 rpm. However, the average surface ' $h$ ' on the rotor is 16.2 W/m<sup>2</sup>K and 24.7 W/m<sup>2</sup>K at 482 rpm and 964 rpm respectively, Fig. 3.4a, b. A wide range in ' $h$ ' value is observed on the rotor surface, which is due to the presence of one fin and one air-vent on the rotor surface, which has been introduced for design manager study which is not within the scope of this study.

The Nusselt number and heat transfer coefficient in the air gap is determined using heat flux and the temperature difference between the air gap fluid volume and rotor surface. The calculated Taylor number ( $Ta$ ) for the two simulation conditions is 6.7 and 13.4 which is less than 41. Therefore no vortices are expected to be formed inside the airgap and the flow is laminar.

The Nusselt number for this type of flow is approximately 2 and the heat transfer in the gap can be considered as conduction. With further increase in the angular speed of the motor, the ' $Ta$ ' will also increase and can exceed the critical value at an extremely higher speed of 4500 rpm or more which is higher than the operating range of this machine., shows the simulation values for the ' $Nu$ ' and ' $h$ ' which are

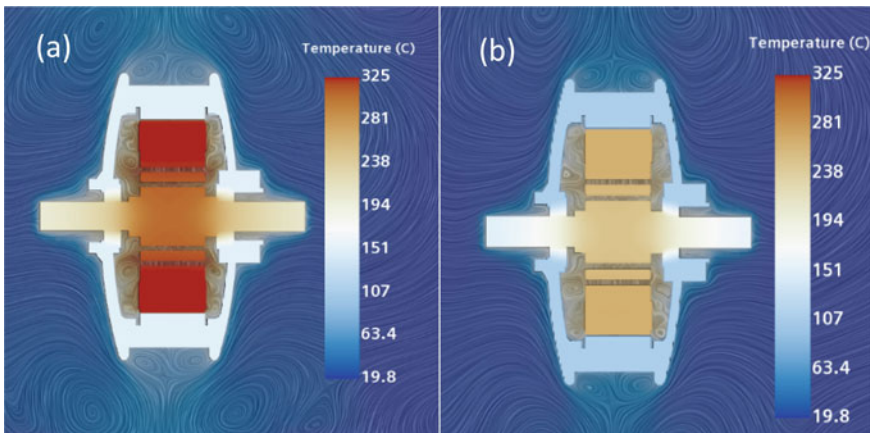


**Fig. 3.3** Shows the temperature distribution on a section plane at 180 W heat load in the hub motor **a** the temperature profile for 482 rpm **b** the temperature profile at 964 rpm

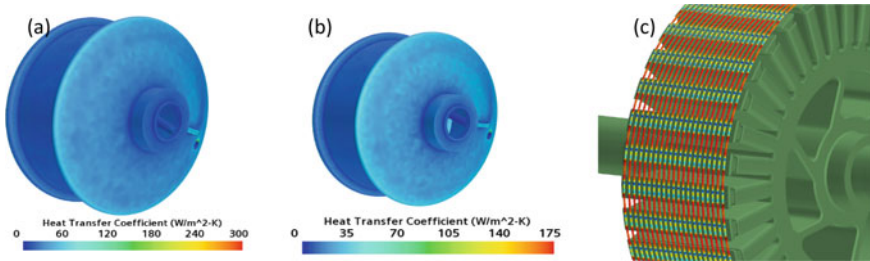


**Fig. 3.4** Shows the heat transfer coefficient on the surface of the rotor and air gap fluid flow, **a, b** the rotor surface heat transfer coefficient at 482 rpm and 964 rpm respectively **c** shows the streamline of the fluid particle in the air-gap at 482 rpm

**Table 3.1** Shows the Nu, h and  $h_{avg}$  calculated numerically and with the correlations

Quantities	482 rpm		964 rpm	
	Simulation	Correlation	Simulation	Correlation
Nu (air gap)	1.77	2.0088	1.93	2.009
h (air-gap, W/m <sup>2</sup> K)	46.3	50.23	50.3	50.23
$h_{avg}$ (rotor surface, W/m <sup>2</sup> K)	16.2	–	24.7	–

numerically determined and compared with the correlations values. The correlations in both cases show a variation of 8.5% because the correlation for Nusselt number in laminar flow only depends on the rotor and stator radius. In fact the Nusselt number depends on the angular velocity of the fluid flow which resulted in slight variation in the values calculated numerically with that of correlations. These values shows an overall good agreement (Table 3.1).

### 3.4 Conclusion

In the current work, the conjugate heat transfer across the motor from the winding to the ambient temperature was studied, providing detailed insight into the heat transfer and fluid flow inside the air-gap. The model and assessment predict overall heat transfer and Nusselt number in the air gap with good agreement to the correlation values. The simulation results also point out the rotor surface heat transfer coefficient which will be taken into consideration as boundary conditions for the further studies. This validation study gives an insight and understanding of the heat transfer and fluid dynamics which serves as a baseline results for further development of advanced aerodynamic cooling for the wheel hub motors. The baseline design shows that the motor may fail if it works at low rpm with high torque due to the high temperature of the coils. Next stage of the research study will be mainly focussing on the experimental validation of the simulation model for a constant power loss



and also investigate the effect of design modifications with the fins and air-vents on the surface of the rotor. Additionally, the optimization of the air-vents for maximum heat transfer from the windings to the ambient air could significantly bring down the temperature hike in the windings.

## References

1. B. Gombert, R. Fischer, W. Heinrich, Wheel-hub motors. Criteria of construction and vehicle integration; Elektrische Radnabenmotoren. Konstruktionskriterien und Fahrzeugintegration' (2010)
2. J. Huang et al., A hybrid electric vehicle motor cooling system—Design, model, and control. *IEEE Trans. Veh. Technol.* **68**(5), 4467–4478 (2019)
3. Z. Huang, F. Marquez, M. Alakula, J. Yuan, Characterization and application of forced cooling channels for traction motors in HEVs, in *2012 XXth International Conference on Electrical Machines* (2012), pp 1212–1218
4. L. Wang, W. Haifeng, Steady-state thermal simulation of the stator coil of the evaporative inner cooling system in wind turbines, in *2012 IEEE 6th International Conference on Information and Automation for Sustainability*, 2012, pp. 248–251
5. S. Nategh et al., A review on different aspects of traction motor design for railway applications. *IEEE Trans. Ind. Appl.* **56**(3), 2148–2157 (2020)
6. M. Fasil, D. Plesner, J.H. Walther, N. Mijatovic, J. Holbøll, B.B. Jensen, Numerical and experimental investigation of heat flow in permanent magnet brushless DC hub motor. *SAE Int. J. Altern. Powertrains* **4**(1), 46–57 (2015)
7. T. Jokinen, V. Hrabovcova, J. Pyrhonen, *Design of Rotating Electrical Machines*. John Wiley & Sons, 2013.
8. D.A. Howey, P.R. Childs, A.S. Holmes, Air-gap convection in rotating electrical machines. *IEEE Trans. Ind. Electron.* **59**(3), 1367–1375 (2010)
9. R. Wrobel, P.H. Mellor, N. McNeill, D.A. Staton, Thermal performance of an open-slot modular-wound machine with external rotor. *IEEE Trans. Energy Convers.* **25**(2), 403–411 (2010)
10. M.L. Hosain, R.B. Fdhila, K. Rönnerberg, Air-gap flow and thermal analysis of rotating machines using CFD. *Energy Procedia* **105**, 5153–5159 (2017)
11. G.I. Taylor, Distribution of velocity and temperature between concentric rotating cylinders. *Proc. R. Soc. Lond. Ser. Math. Phys. Sci.* **151**(874), 494–512 (1935)
12. Y. Yang et al., Thermal management of electric machines. *IET Electr. Syst. Transp.* **7**(2), 104–116 (2017)

**Open Access** This chapter is licensed under the terms of the Creative Commons Attribution 4.0 International License (<http://creativecommons.org/licenses/by/4.0/>), which permits use, sharing, adaptation, distribution and reproduction in any medium or format, as long as you give appropriate credit to the original author(s) and the source, provide a link to the Creative Commons license and indicate if changes were made.

The images or other third party material in this chapter are included in the chapter's Creative Commons license, unless indicated otherwise in a credit line to the material. If material is not included in the chapter's Creative Commons license and your intended use is not permitted by statutory regulation or exceeds the permitted use, you will need to obtain permission directly from the copyright holder.

